Resolution of Homonymous Visual Field Loss Documented with Functional Magnetic Resonance and Diffusion Tensor Imaging

Masaki Yoshida, MD, PhD, Masahiro Ida, MD, Thien Huong Nguyen, MD, PhD, Marie-Therese Iba-Zizen, MD, Luc Bellinger, MD, Jean Louis Stievenart, MD, Takehiko Nagao, MD, Shinsuke Kikuchi, MD, Takaaki Hara, MD, Takuya Shiba, MD, Kenji Kitahara, MD, PhD, and Emmanuel Alain Cabanis, MD, PhD

Abstract: A 68-year-old man developed right homonymous hemianopic paracentral scotomas from acute infarction of the left extrastriate area. He was studied over the ensuing 12 months with visual fields, conventional MRI, functional MRI (fMRI), and diffusion tensor imaging (DTI). As the visual field defect became smaller, fMRI demonstrated progressively larger areas of cortical activation. DTI initially showed that the lesioned posterior optic radiations were completely interrupted. This interruption lessened in time and had disappeared by one year after onset. fMRI and DTI are innovative measures to follow functional and structural recovery in the central nervous system. This is the first reported application of these imaging techniques to acute cerebral visual field disorders.

(*J Neuro-Ophthalmol* 2006;26: 11–17)

Cerebral lesions that involve the retrochiasmal visual pathway can cause contralateral visual field defects. As many as 50% of patients with such lesions show at least some spontaneous recovery (1). This recovery is normally assessed with visual field testing.

Functional magnetic resonance imaging (fMRI) is a non-invasive technique that can be used to investigate brain function with good spatial and temporal resolution. fMRI indirectly monitors modulated local blood oxygenation levels associated with neural activity (2). The effectiveness of fMRI for assessing visual dysfunction, especially that caused by stroke, has not been confirmed.

Departments of Radiology (MI) and Neurology (TN), Tokyo Metropolitan Ebara Hospital, Tokyo, Japan; Department of Ophthalmology (MY, SK, TH, TS, KK), Jukei University School of Medicine, Tokyo, Japan; Department of Neuro-Imaging (TN, M-TI-Z, LB, JLS, EAC), Centre Hospitaloer National d'Ophtalmologie des XV-XX, Paris, France.

Address correspondence to Masaki Yoshida, MD, PhD, Department of Ophthalmology, The Jikei University School of Medicine, 3-25-8 Nishi-shinbashi Minato-ku Tokyo 105-0003 Japan; E-mail: masakiy@jikei.ac.jp

Diffusion tensor imaging (DTI) is a recently developed technique in which diffusion anisotropy is quantitatively measured as the incoherent directional distribution of free water diffusibility on each voxel as a diffusion ellipsoid (3). Because this ellipsoid closely resembles axonal fibers, a fiber tract map can be created to display the axonal network when the shape and orientation of ellipsoids are similar between neighboring voxels (4).

We report a patient with right homonymous hemianopic paracentral scotomas in whom MRI showed an acute infarct involving the left occipital lobe. As the visual field defects gradually improved, fMRI showed improved ipsilateral cortical activation and DTI showed reconstitution of the lesioned optic radiations.

CASE REPORT AND STUDY METHODS

Clinical Features

A 68-year-old man with atrial fibrillation who had been treated with anticoagulation therapy reported the sudden onset of cloudiness of the right visual field. Forty-eight hours later, ophthalmologic examination disclosed a best-corrected visual acuity of 20/25 OD and 20/20 OS. Right homonymous hemianopic paracentral scotomas were observed with Goldmann kinetic perimetry (Fig. 1). The patient then underwent the following serial imaging studies:

Conventional MRI

MRI was performed with a 1.5-T clinical scanner (Magnetom Vision, Siemens, Erlangen, Germany) with the use of a head coil. Three-dimensional time-of-flight magnetic resonance (MR) angiography (3-D TOF-MRA) was also performed. After these conventional MR data were acquired, fMRI, DTI, and 3-D inversion-recovery T1-weighted anatomical imaging (magnetization prepared rapid acquisition gradient-echo [MPRAGE]) were performed. The MPRAGE images were obtained with the following

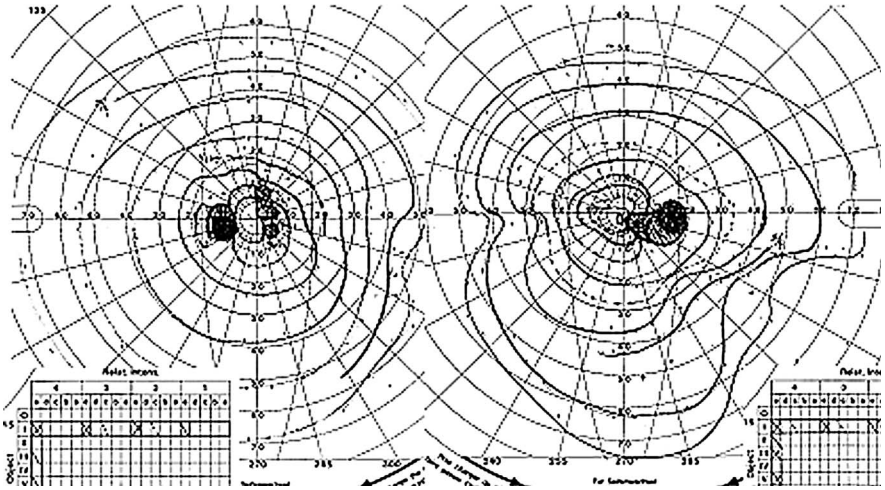

FIG. 1. Goldmann perimetry performed two days after stroke shows right homonymous hemianopic scotomas.

parameters: 10.3 milliseconds/300 milliseconds/300 milliseconds/1 (repetition time [TR]/echo time [TE]/spin lattice relaxation time [T1]/excitations); flip angle 15°; matrix 256 × 256; field of view 210 × 210 mm; slice thickness 2.5 mm; and number of sections 80.

Functional MRI

fMRI was performed with a single-shot, gradient-echo, echo-planar sequence with the following parameters: echo time 60 milliseconds, repetition time 3000 milliseconds, flip angle 90°; matrix 64 × 64; field of view 210–240 mm, slice thickness 4 mm. Twenty-five axial images, including images of the entire brain parallel to the calcarine fissure, were obtained.

For fMRI, all stimuli were generated on a personal computer using homemade software. A liquid crystal display projector (TLP411J, Toshiba Corp., Tokyo, Japan) with a resolution of 800 × 600 pixels was used to project these stimuli onto a front-projection screen. The patient viewed the stimuli via an adjustable mirror angled at 45° to the line of sight.

For the stimulation condition, a black-and-white checkerboard reversing at 8 Hz was used. Each square of the checkerboard subtended a visual angle of 0.75° in height and width. The mean luminance of the checkerboard projection was 75 candela/m^2 and its contrast was close to 90%.

Three types of stimuli were presented. In the resting phase, a central fixation point was projected on a gray background with the same mean luminance as the checkerboard. In succession, a horizontal wedge-shaped checkerboard with 30° of polar angle was projected on the right visual field, and a round, centrally-positioned checkerboard subtending 15° of visual angle was projected onto the central fixation point.

Each experimental run consisted of the acquisition of 120 volumes, with volume acquisition for three seconds, giving a total run time of six minutes. The 120 volumes were divided into 15 blocks of eight volumes, corresponding to five iterations of three phases; a rest phase was followed by an Activation 1 phase and an Activation 2 phase. Each phase contained eight volumes for a duration of 24 seconds. In the first block – the rest phase – the fixation point was projected. In the second and third blocks – the Activation 1 and 2 phases – the wedge-shaped checkerboard on the right visual field and round checkerboard were presented. In this binocular vision investigation, the subject's task was to fix on the central dot during the rest and activation phases.

Diffusion Tensor Imaging

DTI was performed with a single-shot, spin-echo, echo-planar sequence with the following parameters: echo time 100 milliseconds, repetition time 4000 milliseconds; matrix 128 × 128 interpolated 256 × 256; field of view 220 × 220 mm; slice thickness 20 interleaved contiguous 5 mm; diffusion gradient 6 directions with the b 1000 s/mm as the peak and also b 0 s/mm for T2-weighted images. The total run time of DTI was 96 seconds with three excitations.

Data Analysis

The fMRI data were analyzed with a conventional personal computer (Windows 2000 operating system, Pentium IV 1.5-GHz processor, 768 megabytes random access memory), our own Image Calculator V0.44 software, and the SPM2 software package (Wellcome Department of Imaging Neuroscience, University College London, London, UK) (5). The images were transformed with Image Calculator V0.44 software into analyze format for further treatment with SPM2 software.

Functional images of each experiment were realigned and transformed into the anatomical space defined by Talairach and Tournoux (6). These two steps were

performed under standard parameters (default settings) suggested for the SPM2 software. The images were spatially smoothed with a Gaussian filter (full width at half maximum = 6 mm in three directions). A box-car design with the hemodynamic response function (hrf) was used. Two comparisons were made for each experiment: Contrast I, in which the first block (fixation point only, R) was compared with the second block (wedge-shaped right visual field stimulation, Activation 1) to evaluate residual left cortical function, and Contrast II, in which the first block (fixation point only, R) was compared with the third block (a centrally-positioned circle subtending 15° of visual angle, Activation 2) to compare affected left cortical function with unaffected right cortical function. For statistical comparison, differences with corrected P values < 0.05 with multiple testing at the voxel level and the 50-voxel extended threshold were considered significant.

The DTI data were analyzed with the same personal computer, VOLUME-ONE V1.56 software program, the diffusion TENSOR visualizer (dTV) V1.5 software program (7). These software programs were developed by the Image Computing and Analysis Laboratory, Department of Radiology, University of Tokyo (http://www.ut-radiology.umin.jp/). The distortion of raw data images (7) was not corrected before DTI data were analyzed. Practical analysis of these software programs is demonstrated by example in a healthy subject (Fig. 2). To visualize the optic radiations, we drew a region of interest as a seed on green areas, which corresponded to the major eigenvector perpendicular to this plane resulting from dTV software (Fig. 2A) on a coronal section between the trigone and the posterior horn of the lateral ventricle (Fig. 2B). To trace axonal projections, the tensor was tracked and lines were drawn in both antegrade and retrograde directions in 3-D space from seeds along the major eigenvector. The optic radiations were shown to reach both occipital poles (Fig. 2C).

RESULTS

Visual Fields

Goldmann kinetic perimetry performed one month after onset disclosed marked improvement of the right homonymous visual field deficit (Fig. 3).

Conventional MRI

On initial imaging two days after onset, the lesion in the left occipital lobe appeared as a high-intensity area in an extrastriate cortical area on diffusion-weighted imaging (DWI) (Fig. 4A), FLAIR (Fig. 5A), and T2-weighted images. On the ninth day after onset, repeat MRI showed lower signal intensity on DWI (Fig. 4B) and a smaller area of high-intensity signal on FLAIR (Fig. 5B).

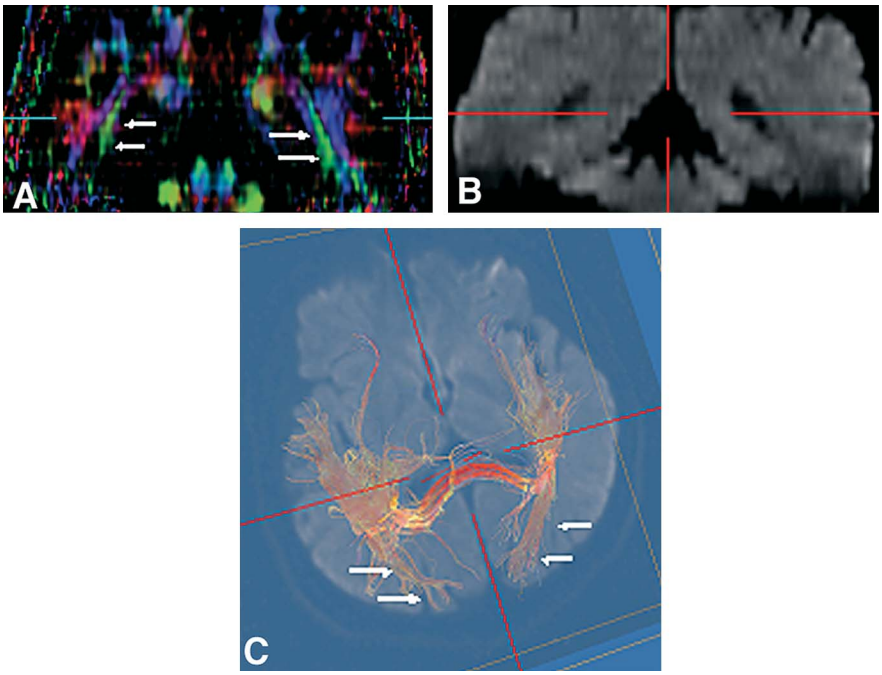

FIG. 2. Diffusion tensor imaging (DTI) fiber tracking of optic radiations in a healthy subject. We drew a region of interest as a seed on green areas (white arrow) which correspond to the major eigenvector direction perpendicular to this plane **(A)** and on a coronal section between the trigone and the posterior horn of the lateral ventricle **(B)**. The tensor was tracked, and lines were drawn in both antegrade and retrograde direction in three-dimensional space; the optic radiations are shown to reach both occipital poles **(C)**.

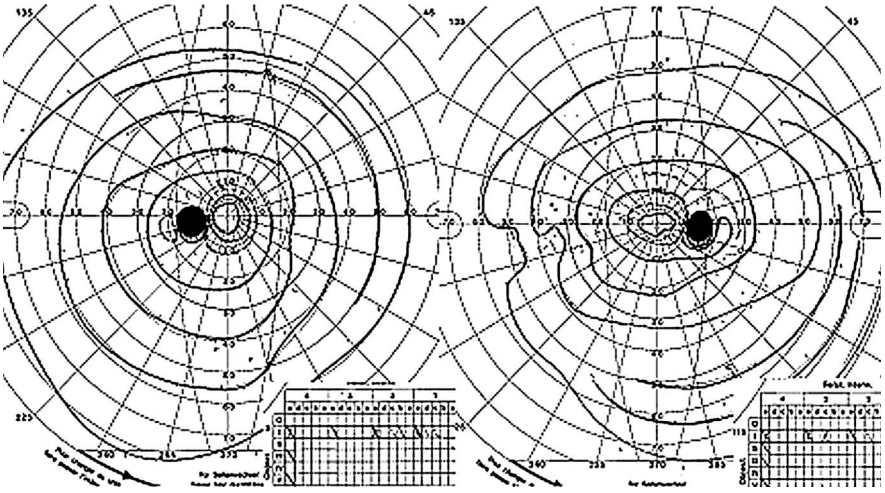

FIG. 3. Goldmann perimetry performed four weeks after stroke shows marked improvement in visual field defects.

Functional MRI

fMRI data were acquired two days after onset, nine days after onset, 30 days after onset, and one year after onset (Fig. 6). The Contrast I experiment (Fig. 6, top) demonstrated progressively larger areas of left cortical activation (two days after onset, 384 voxels; nine days after onset, 449 voxels; 30 days after onset, 716 voxels; one year after onset, 1540 voxels). The center of activation was displaced from the first acquisition (two days after onset; x/y/z: -12/-90/-4) to a more posterior portion of the Talairach space (6) on the second acquisition (–14/-98 or –100/4), which was consistent with the left occipital pole. The Contrast II experiment (Fig. 6, bottom), designed to simultaneously evaluate the visual cortices of both the affected and unaffected cerebral hemispheres, showed broadest activation two days after onset (two days after onset, 5,979 voxels; nine days after onset, 1,957 voxels; four weeks after onset, 4,109 voxels; one year after onset, 4,580 voxels). The activated visual areas of the unaffected right hemisphere were most diffuse two days after onset, were smallest nine days after onset, and demonstrated consistent increases across sessions. The ratios of the sizes of activated visual areas on the left and right sides demonstrated decreasing asymmetry (two days after onset, L:R ratio = 0.12, 640–5,339 voxels; nine days after onset, L:R ratio = 0.26, 403–1,554 voxels; four weeks after onset, L:R ratio = 0.37, 1109–3,000 voxels; one year after onset, L:R ratio = 0.79, 2,021–2,559).

Diffusion Tensor Imaging

DTI data were analyzed to track the optic radiations two days after onset, nine days after onset, and one year

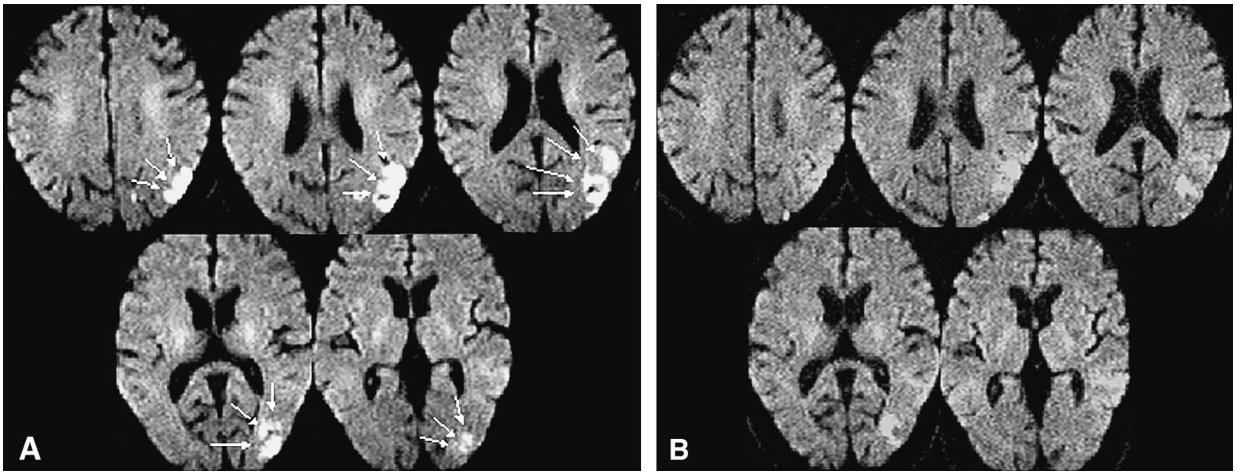

FIG. 4. Axial diffusion-weighted imaging (DWI). **A.** Performed two days after onset, DWI shows a high-intensity area (white arrow) corresponding to the left occipital lobe infarct. **B.** Performed nine days after onset, DWI shows decreased signal intensity and smaller areas of hyperintensity as compared to **A.**

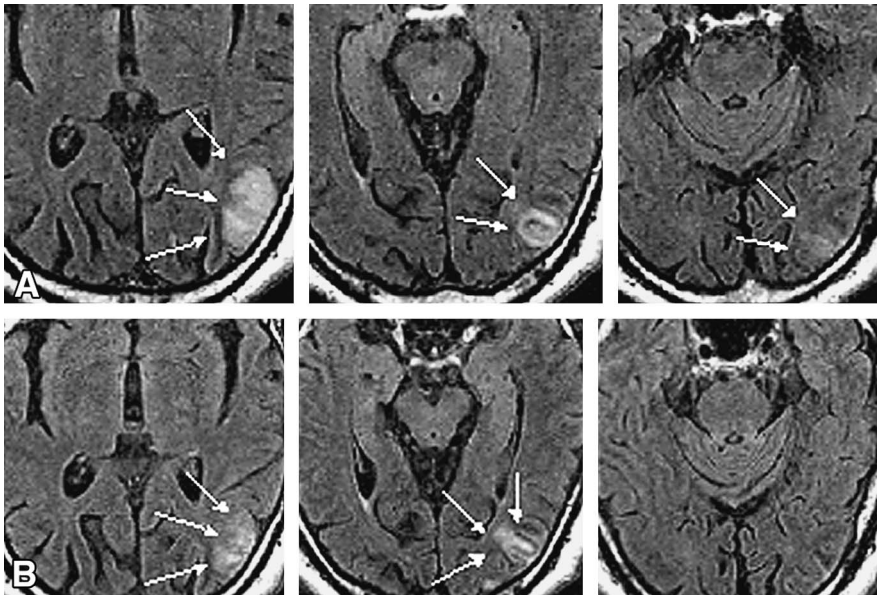

FIG. 5. FLAIR imaging. **A.** Performed two days after onset, it shows high signal (white arrow) in the same area as seen on diffusion-weighted imaging (DWI) (Fig. 4). **B.** Performed nine days after onset, it shows decreased hyperintensity as compared to **B.**

after onset (Fig. 7). On the initial study, the tracked optic radiation reached the occipital pole on the right side (Fig. 7A, black arrows), but fiber tracking was completely interrupted on the left side at the area of high DWI signal intensity corresponding to the cortical lesion (Fig. 7A: white arrow). Nine days after onset, fiber tracking was interrupted to a lesser degree at the left cortical lesion (Fig. 7B, white arrow). One year after onset, fiber tracking demonstrated no interruption and no high-intensity areas on DWI (Fig. 7C).

DISCUSSION

Although several papers have described fMRI and DTI findings in patients with cerebral visual field disorders (8,9), we are not aware of any reports of longitudinal fMRI or DTI studies of acute cerebral infarction producing homonymous hemianopia.

In our patient, fMRI results showed progressive increase in the activated areas of the affected left hemisphere consistent with functional recovery and progressive decrease in the activated areas in the unaffected right hemisphere associated with recovery. Metabolic change after acute stroke can result in widespread areas of cortical hyperexcitability in regions structurally connected to the lesion in both hemispheres as a consequence of down-regulation of the gamma amino butyric acid (GABA) receptor subunit and a decrease in GABAergic inhibition (10), resulting in increased diffuse blood oxygenation level-dependent signals. When comparing task-related brain activation in the acute and chronic phases of motor recovery after stroke, positron emission tomography (11,12) and fMRI (13,14) data demonstrate greater and more widespread brain activation in early stages than in later stages. This widespread cortical activation, including the bilateral primary motor cortices (M1), decreases with recovery (13). Patients with poorer recovery tend to recruit more cortical regions during motor performance, and motor recovery is negatively correlated with task-related cortical activation (15).

In the Contrast II experiment, the activated visual areas of the healthy right hemisphere were most diffuse 48 hours after onset. This finding suggests that the affected left hemisphere recruits more cortical regions to the healthy right hemisphere during the acute phase.

In our patient, the DTI fiber tract map of the left optic radiation was interrupted at the area of infarction corresponding to an area of high signal intensity that appeared like a white cloud caused by cellular and/or stromal edema within the acute infarction. Acute cerebral infarction causes reduced diffusion anisotropy (16), which can produce a fiber-tracking defect. Consistent with disappearing areas of high signal intensity, fiber tract maps one year after onset showed an intact optic radiation in the infarcted left hemisphere.

Although several studies have evaluated axonal function after stroke using fiber tract mapping (17,18), this technique requires further refinement before it can be used to quantitatively evaluate axonal dysfunction and its consequences. Nevertheless, fiber tract maps showed that the infarcted area in our patient was located on the main trajectory of the left optic radiation, which was morpologically reconstituted one year after onset.

Our results suggest that fMRI and DTI are useful for investigating cerebral visual field disorders, including those in the acute phase.

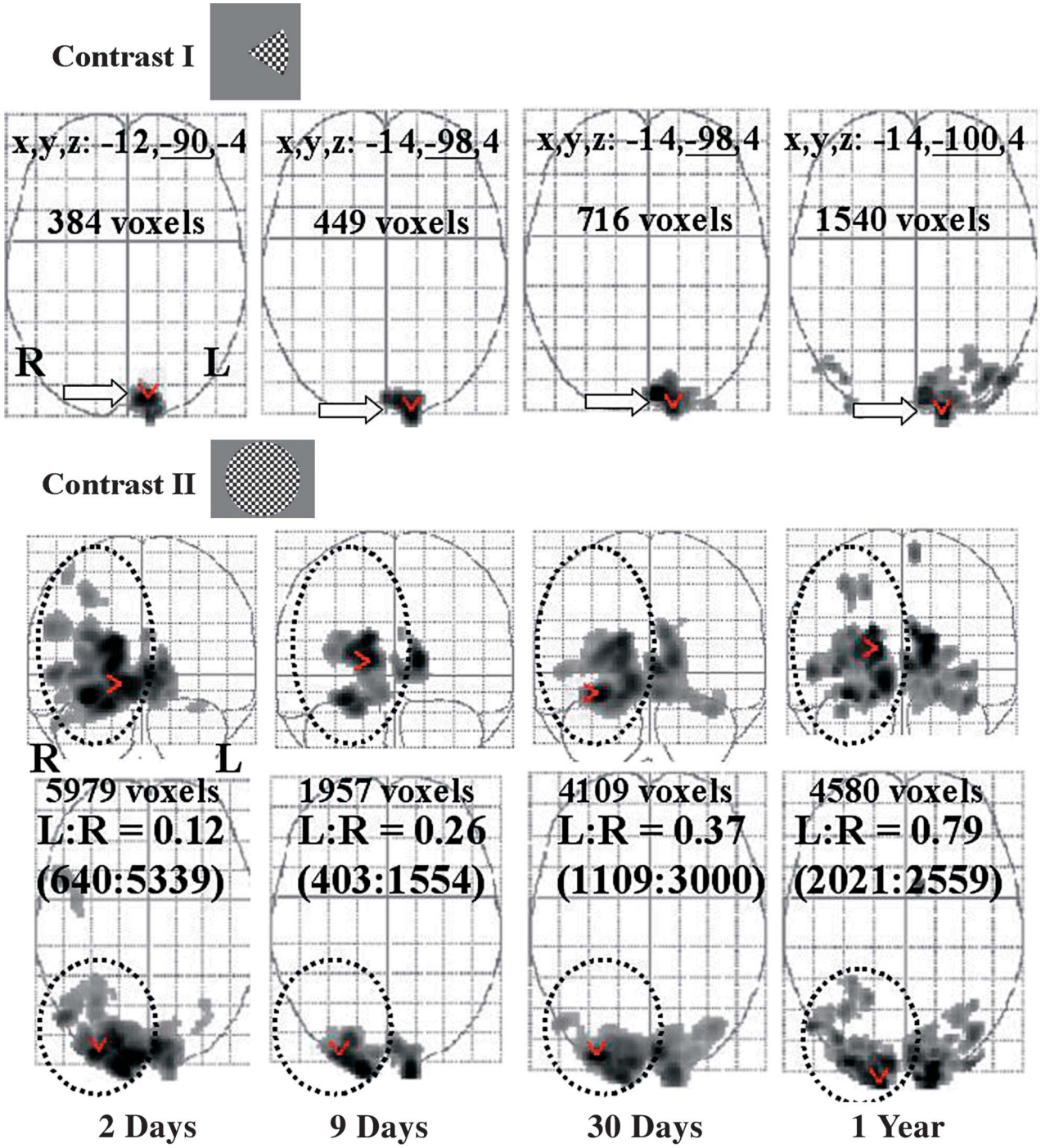

FIG. 6. Longitudinal functional MRI (fMRI) results. Top: Contrast I experiment demonstrates progressively larger areas of activation corresponding to the left striate cortex. On the second acquisition, the center of activation is displaced to a more posterior portion of the Talairach space as compared to the first acquisition. Bottom: Contrast II experiment shows broadest activation two days after onset. The activated visual areas of the unaffected right hemisphere are most diffuse two days after onset, smallest nine days after onset, and demonstrate consistent increases thereafter. The ratios of the sizes of activated visual areas of the two cerebral hemispheres demonstrates decreasing asymmetry.

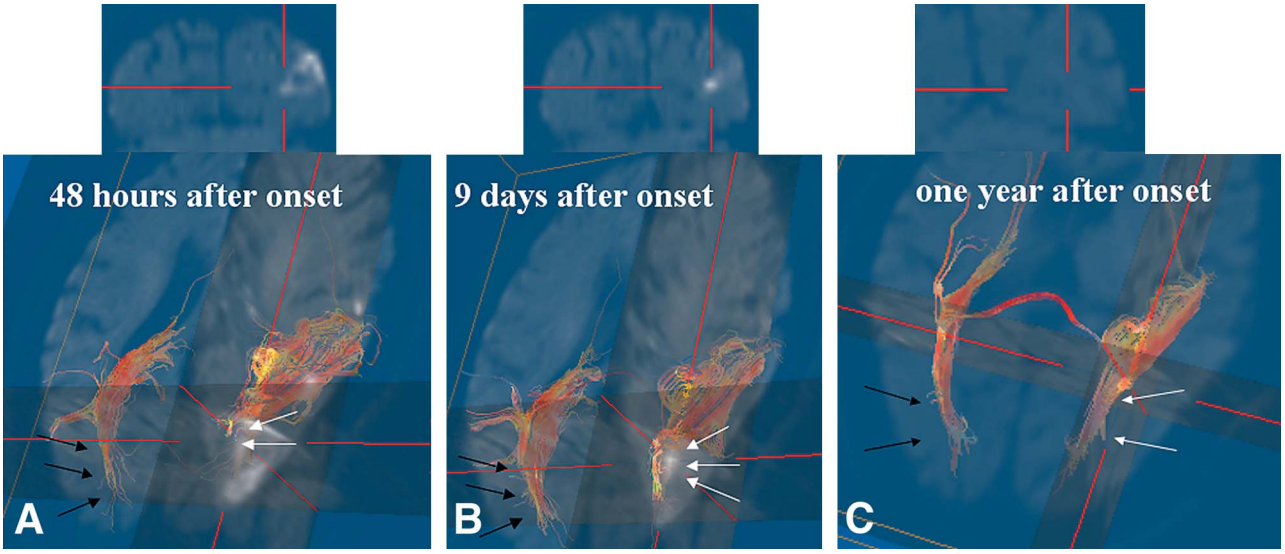

FIG. 7. Diffusion Tensor Imaging (DTI) performed two days after onset **(A)**, nine days after onset **(B)**, and one year after onset **(C)**. **A.** The optic radiation reaches the occipital pole in the right hemisphere (black arrow) but is completely interrupted in the left hemisphere, corresponding to a high-intensity area that appears like a white cloud caused by local edema (white arrow). **B.** The left optic radiations are interrupted to a lesser extent at the left cortical lesion (white arrow). **C.** There is no longer any interruption in the left optic radiations.

Acknowledgment

This work was performed under an agreement of cooperation between The Pierre and Marie Curie University (Paris, France) and The Jikei University School of Medicine (Tokyo, Japan).

REFERENCES

1. Panbakian ALM, Kennard C. Can visual function be restored in patients with homonymous hemianopia? *Br J Ophthalmol* 1997;81: 324–8.
2. Ogawa S, Tank DW, Menon R, et al. Intrinsic signal changes accompanying sensory stimulation: Functional brain mapping with magnetic resonance imaging. *Proc Natl Acad Sci USA* 1992;89: 5951–5.
3. Chenevert TL, Brumberg JA, Pipe JG. Anisotropic diffusion in human white matter: demonstration with MR technique in vivo. *Radiology* 1990;177:401–5.
4. Melhem ER, Mori S, Mukundan G, et al. Diffusion tensor MR imaging of the brain and white matter tractography. *Am J Roentgenol* 2002;178:3–16.
5. Friston KJ, Holmes AP, Worsley KJ, et al. Statistical parametric maps in functional imaging: A general linear approach. *Hmn Brain Map* 1995;2:189–210.
6. Talairach J, Tournoux P. Co-Planar Stereotaxic Atlas of the Human Brain: An Approach to Medical Cerebral Imaging. New York: Thieme; 1988.
7. Masutani Y, Aoki S, Abe O, et al. MR diffusion tensor imaging: recent advantage and new techniques for diffusion tensor visualization. *Eur J Radiol* 2003;46:53–66.
8. Kleiser R, Wittsack J, Niedeggen M, et al. Is V1 necessary for conscious vision in areas of relative cortical blindness? *Neuroimage* 2001;13:654–61.
9. Goebel R, Muckli L, Zanella FE, et al. Sustained extrastriate cortical activation without visual awareness revealed by fMRI studies of hemianopic patients. *Vision Res* 2001;41:1459–74.
10. Neuman-Haefelin T, Stainger JF, Redecker C, et al. Immunohistochemical evidence for dysregulation of the GABAergic system ipsilateral to photochemically induced cortical infarcts in rats. *Neuroscience* 1998;87:871–9.
11. Marshall RS, Perera GM, Lazar RM, et al. Evolution of cortical activation during recovery from corticospinal tract infarction. *Stroke* 2000;31:656–61.
12. Calautti C, Leroy F, Guincester JY, et al. Dynamics of motor network overactivation after striatocapsular stroke: a longitudinal PET study using a fixed-performance paradigm. *Stroke* 2001;32:2534–42.
13. Ward NS, Brown MM, Thompson AJ, et al. Neural correlates of motor recovery after stroke: a longitudinal fMRI study. *Brain* 2003; 126:2476–9.
14. Horton JC, Hoyt WF. Quadrantic visual field defects. A hallmark of lesions in extrastriate (V2/V3) cortex. *Brain* 1991;114:1703–18.
15. Ward NS, Brown MM, Thompson AJ, et al. Neural correlates of outcome after stroke: a cross-sectional fMRI study. *Brain* 2003;126: 1430–48.
16. Sorensen AG, Wu O, Copen WA, Davis TL, et al. Human acute cerebral ischemia: detection of changes in water diffusion anisotropy by using MR imaging. *Radiology* 1999;212:785–92.
17. Kunimatsu A, Aoki S, Masutani Y, et al. Three-dimensional white matter tractography by diffusion tensor imaging in ischaemic stroke involving the corticospinal tract. *Neuroradiology* 2003;45:532–35.
18. Kunimatsu A, Aoki S, Masutani Y, et al. The optimal trackability threshold of fractional anisotropy for diffusion tensor tractography of the corticospinal tract. *Magn Res Med Sci* 2004;3:11–7.